

Accurate, fast, and robust centre localisation for images of semiconductor components

Fabian Timm^{a,b} and Erhardt Barth^a

^aInstitute for Neuro- and Bioinformatics, University of Lübeck
Ratzeburger Allee 160, D-23538 Lübeck, Germany

^bPattern Recognition Company GmbH
Maria-Goeppert-Strasse 1, D-23562 Lübeck, Germany

ABSTRACT

The problem of circular object detection and localisation arises quite often in machine vision applications, for example in semi-conductor component inspection. We propose two novel approaches for the precise centre localisation of circular objects, *e.g.* p-electrodes of light-emitting diodes. The first approach is based on image gradients, for which we provide an objective function that is solely based on dot products and can be maximised by gradient ascend. The second approach is inspired by the concept of isophotes, for which we derive an objective function that is based on the definition of radial symmetry. We evaluate our algorithms on synthetic images with several kinds of noise and on images of semiconductor components and we show that they perform better and are faster than state of the art approaches such as the Hough transform. The radial symmetry approach proved to be the most robust one, especially for low contrast images and strong noise with a mean error of 0.86 pixel for synthetic images and 0.98 pixel for real world images. The gradient approach yields more accurate results for almost all images (mean error of 4 pixel) compared to the Hough transform (8 pixel). Concerning runtime, the gradient-based approach significantly outperforms the other approaches being 5 times faster than the Hough transform; the radial symmetry approach is 12% faster.

Keywords: centre localisation, semiconductor components, optical inspection, calibration, object detection

1. INTRODUCTION

For solving machine vision problems a stepwise approach is often applied, which begins with a rough localisation of the relevant object and is refined in every stage until the relevant objects are detected accurately. Since every stage can usually be computed efficiently and the combination of all stages is powerful and robust to noise, this general technique is favoured in many applications. In the case of LED calibration and inspection, a stepwise approach is applied to first identify rough regions of interest (see Fig. 1). Afterwards, in a refinement step, the exact centre of the relevant object is evaluated and used for system calibration, which has to be very accurate for most semiconductor inspection tasks such as the inspection of light emitting devices. Even a slight prediction error (1–5 pixel) of the estimated centre will produce a poor calibration and thus most of the manufactured LEDs will not meet the required quality.

For this work, we assume that at least one step of preprocessing was done such that the image already contains the circular object, *e.g.* an annulus or a circle. Such a preprocessing can be performed by template matching or by using prior knowledge, for example. We here propose two novel approaches for the centre location of a circular object. The first approach is based on image gradients with a novel objective function which has to be maximised. Therefor, we develop a simple and fast iterative algorithm, which is robust to noise and low contrast. The second approach is inspired by the concept of isophotes, for which we derive an objective function based on the definition of radial symmetry. Geometrically, given the optimal centre, the intensities along a circle with a

Further author information: (send correspondence to FT)

FT: timm@inb.uni-luebeck.de, +49 (0) 451 / 500 55 13

EB: barth@inb.uni-luebeck.de, +49 (0) 451 / 500 55 13

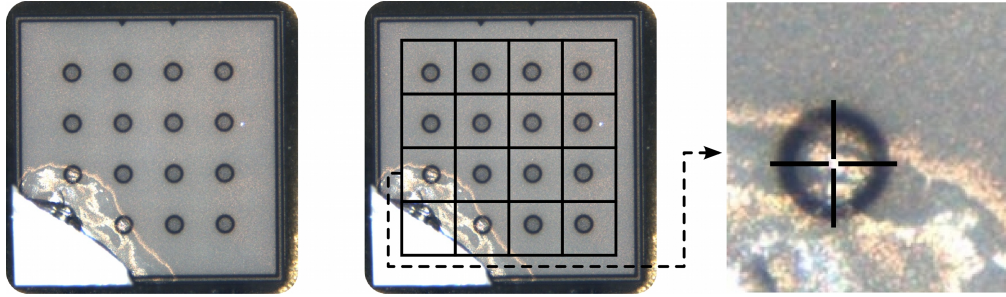


Figure 1. For images of semiconductor components, *e.g.* LEDs, often a stepwise approach is applied. First, the LED (left) is roughly divided by a fixed grid (middle); then, the centres are detected accurately (right) and used for further processing, *e.g.* calibration or inspection. Especially for calibration, a precise centre localisation is necessary.

certain radius from that centre vary only slightly. Therefore, the centre is the location where the mean variation of intensities over several radii reaches its minimum.

We apply the two approaches to synthetic images as well as real world images, and we compare to an approach based on the Hough transform.

2. CENTRE LOCALISATION

One of the well-known approaches for the detection of lines, circles, and ellipses is the Hough transform.¹⁻⁴ The Hough transform approaches are voting-based techniques and the motivating idea is that each sample, *e.g.* a contour point obtained by edge detection or a point in a binary image, indicates its contribution to a globally consistent solution. Over the last 35 years, several modifications have been proposed to improve the Hough transform in terms of accuracy and efficiency.^{3,5,6} A good survey on Hough transforms has been proposed by Illingworth and Kittler.⁷ However, several comparative studies show that the information about edges in an image is not sufficient to detect circles accurately, especially in the presence of noise.^{8,9} To overcome this problem, Ceccaralli *et al.* proposed a method that avoids the detection of edges but tries to detect a circular object by using a template matching mechanism that retains the information about pixel intensity.¹⁰ In particular, template matching is performed between the direction of the gradient at each image position and the gradient direction of an ideal circle whose radius varies in a given interval. However, template matching is often computationally inefficient and depends on the quality of the template and the noise level.

Furthermore, isophote properties have been used for object detection¹¹ and eye centre location.¹² The latter employs a voting scheme like the Hough transform. For every pixel, the centre of the osculating circle of the isophote is computed from smoothed derivatives of the image brightness, so each pixel can provide a vote for its own centre. However, these voting-based approaches are also inefficient and lead to the problem of analysing the voting-space, which might contain more than one maximum. Then, the correct optimum cannot be identified easily. Moreover, the derivatives of the image brightness can be affected by noise, especially for low contrast images. In this case, our gradient-based approach might be influenced as well, but the performance will degenerate to a lesser extent as shown by our experiments.

2.1 Edge-based approach

Here, we use the Hough transform for the detection of a circle or an annulus in the image and apply the following standard steps to obtain the centre of the object (see Fig. 2): (i) low-pass filtering to reduce noise, (ii) edge detection to obtain the object's contour, (iii) computing the accumulator array in a predefined space, and (iv) evaluating the maximum of the accumulator array. Since we assume that the circular object is completely located inside the image, the accumulator array is evaluated for $c_x \in [1, W]$, $c_y \in [1, H]$, and $r \in [1, 0.5 \times \min(W, H)]$. The only remaining parameter to be determined is the accuracy in each dimension of the accumulator, which we set to 1 in order to achieve pixel accuracy. For the edge detection, we apply the Canny algorithm with standard parameters to obtain contour points.

For images containing a circle we seek for the total maximum in the accumulator space, whereas for images containing an annulus we seek for two maximum values with significantly different radii in order to be more robust. For the Hough transform approach as well as for the following approaches, the input image is smoothed by convolution with a Gaussian filter ($5 \times 5, \sigma = 1$).

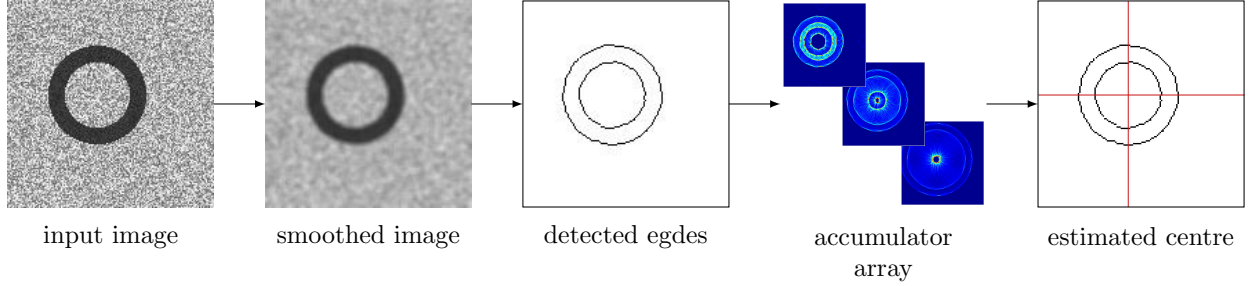


Figure 2. Centre localisation based on the Hough transform. First, the input image is smoothed for noise reduction, then an edge detection algorithm is applied in order to obtain contour points. Based on the contour points, the accumulator arrays are determined by the Hough transform. The accumulator position with the maximum value is then used as estimated centre.

2.2 Gradient-based approach

Another way of detecting the centre of a circular object in a geometric way is to use image gradients. Therefore, we analyse the orientation of the gradient at positions of high variances of grey values, *e.g.* edges and corners. The normalised difference vector between a potential centre \mathbf{c} and a contour point \mathbf{x}_i should have the same orientation (except for the sign) as the gradient \mathbf{g}_i at \mathbf{x}_i if \mathbf{c} is the true centre (see Fig. 3).

We quantify this by computing the dot product between the normalised difference vectors and the unnormalised gradients \mathbf{g}_i . The optimal centre \mathbf{c}^* of a circular object in an image with N pixels at positions \mathbf{x}_i , $i \in \{1, \dots, N\}$, is then given by

$$\mathbf{c}^* = \arg \max_{\mathbf{c}} \{J(\mathbf{c})\} , \quad (1)$$

$$J(\mathbf{c}) = \frac{1}{N} \sum_{i=1}^N (\mathbf{d}_i^T \mathbf{g}_i)^2 , \quad \mathbf{d}_i = \frac{\mathbf{x}_i - \mathbf{c}}{\|\mathbf{x}_i - \mathbf{c}\|_2} . \quad (2)$$

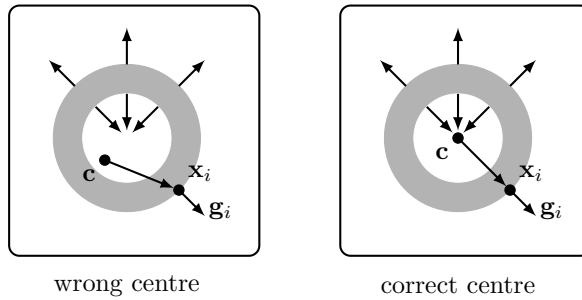


Figure 3. Gradient-based approach for centre localisation. On the left the centre \mathbf{c} is located such that the difference vector $(\mathbf{x}_i - \mathbf{c})$ is different from the absolute orientation of the gradient vector \mathbf{g}_i at position \mathbf{x}_i . Thus the dot product between each difference vector and its gradient vector \mathbf{g}_i is large only for few positions \mathbf{x}_i ; whereas on the right the centre is located correctly and the sum of dot products reaches its maximum.

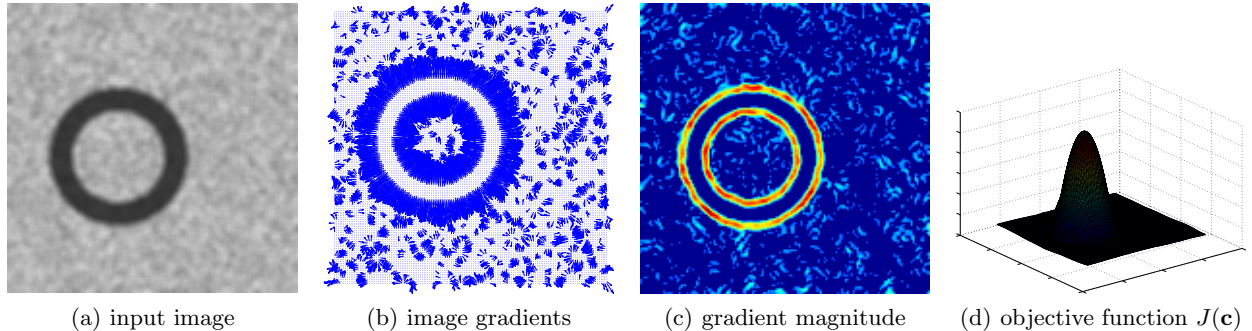


Figure 4. The low-pass filtered input image containing one annulus (a), its image gradients (b), the gradient magnitudes where large values are red/white and small values are blue/black (c), and the corresponding objective function in the xy -plane (d) are shown.

The difference vectors \mathbf{d}_i are scaled to unit length to be invariant to translations. An example of the objective function $J(\mathbf{c})$ is shown in Fig. 4; the objective function will produce smooth results with a significant global maximum (Fig. 4(d)). However, away from the global maximum there might be a plateau with several small local maxima. Thus, for an iterative scheme we need to identify a reasonable starting position in order to guarantee converge; for that, positions with large gradient magnitudes can be used (Fig. 4(c)).

Instead of evaluating J for several centres \mathbf{c} , we propose a gradient ascend approach for determining the maximum. Therefore, the derivatives with respect to $\mathbf{c} = (c_1, c_2)^T$ are

$$\frac{\partial J}{\partial c_k} = \frac{2}{N} \sum_{i=0}^{N-1} \frac{(x_{ik} - c_k) e_i^2 - g_{ik} e_i n_i^2}{n_i^4}, \quad (3)$$

where

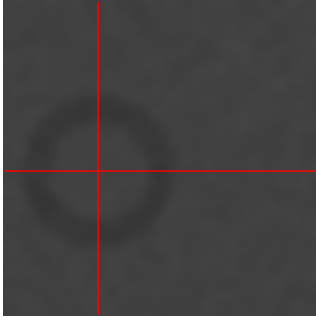
$$\mathbf{g}_i = (g_{i1}, g_{i2})^T, \quad \mathbf{x}_i = (x_{i1}, x_{i2})^T, \quad n_i = \|\mathbf{x}_i - \mathbf{c}\|_2, \quad e_i = (\mathbf{x}_i - \mathbf{c})^T \mathbf{g}_i. \quad (4)$$

The iterative scheme for centre localisation based on image gradients is shown in Algorithm 1. For noisy images with low contrast the area around the global maximum of the objective function (see Fig. 4(d)) might become narrow and the position of the largest magnitude might be outside the convergence area. Therefore, we apply the outer iteration loop m times and determine the centre with the largest objective value as the optimal centre. Within each iteration step we have to compute a stepsize s . Instead of using the Armijo rule¹³ or the Wolfe-Powell rule¹³, which involve the evaluation of $J(\mathbf{c})$ and the gradient several times, we apply the following procedure. First, we normalise the image gradients to unit mean norm in order to limit the dot products. Second, for a fixed number ($n = 10$) of exponentially increasing stepsizes in the experimentally determined interval $[10^{-2}, 10^5]$ we evaluate the objective function $J(\mathbf{c})$. Third, we determine the stepsize, which yields the largest value. The algorithm is fast and yields accurate results even for noisy and low contrast images as shown in Fig. 5. The accuracy and performance of Algorithm 1 can be controlled by changing the values of the number of trials m and the maximum number of iterations t_{\max} for each trial. We can further improve the performance by reducing the number of image gradients, for example, by ignoring all image gradients with magnitude below a (predefined) threshold, *e.g.* the mean magnitude of all image gradients. For the image gradients we simply compute the partial derivatives of the low-pass filtered image I by $\mathbf{g} = (\frac{\partial I}{\partial x}, \frac{\partial I}{\partial y})^T$.

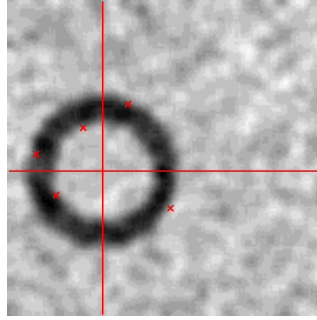
2.3 Symmetry-based approach

In cases of higher image degradations, *e.g.* low contrast in combination with strong noise, the gradient information will not be sufficient for estimating the centre accurately. To overcome this problem, we propose a second approach for centre estimation, which is based on radial symmetry.

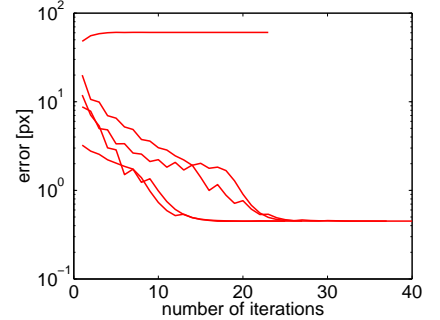
Assume we have an annulus with only few colour variations inside, then there are several isophotes, *i.e.* contours of equal luminance, sharing the same centre. Thus, the mean radial colour variation (standard deviation)



(a) noisy, low contrast image (smoothed)



(b) input image in (a) stretched to full range



(c) Euclidean distance between correct centre and iterated centres

Figure 5. Application of Algorithm 1 with $m = 5$ trials and $t_{\max} = 100$. The detected centre is shown in (a) and (b) by two crossing lines, small crosses in (b) correspond to the 5 initial centres for the iterative algorithm. In (c) the error in pixel between the correct centre and iterated centres is shown. One of the initial centres diverged, whereas the other 4 initial centres converged to the optimum. Convergence is fast, with 30 iterations on average.

Algorithm 1: Iterative centre localisation based on the image gradients.

```

input : pixel positions  $X = \{\mathbf{x}_i\}_{i=1}^N$ ,
         gradients  $G = \{\mathbf{g}_i\}_{i=1}^N$ ,
         number of trials  $m$ ,
         maximum number of iterations  $t_{\max}$ ,
         image width  $W$  and height  $H$ 

output: centre  $\mathbf{c}$ 

for  $i \leftarrow 1$  to  $m$  do
    // position of the  $i$ th largest gradient magnitude
     $\mathbf{c} \leftarrow \text{getInitialCentre}(i)$ 
    for  $j \leftarrow 1$  to  $t_{\max}$  do
         $\mathbf{c}_{old} \leftarrow \mathbf{c}$ 
        // gradient according to Eq. 3
         $\mathbf{g} \leftarrow \text{ComputeGradient}(\mathbf{c}, X, G)$ 
        // see text for explanation
         $s \leftarrow \text{ComputeStepsize}(\mathbf{c}, X, G, \mathbf{g})$ 
        // update centre
         $\mathbf{c} \leftarrow \mathbf{c} + s * \mathbf{g}$ 
        // stop if one of the image borders is reached or the difference
        // compared to the previous step is below a threshold  $\theta$ , e.g.  $\theta = 10^{-3}$ 
        if  $\text{BordersReached}(\mathbf{c}, W, H)$  or  $(\text{norm}(\mathbf{c} - \mathbf{c}_{old}) \leq \theta)$  then
             $\perp$  break
         $C_i \leftarrow \mathbf{c}$ 
        // compute value of objective function Eq. 2 for centre  $i$ 
         $J_i \leftarrow \text{ComputeObjective}(\mathbf{c}, X, G)$ 

    // determine centre with maximum value of objective function
     $\mathbf{c} \leftarrow \arg \max_{C_i} J_i$ 

```

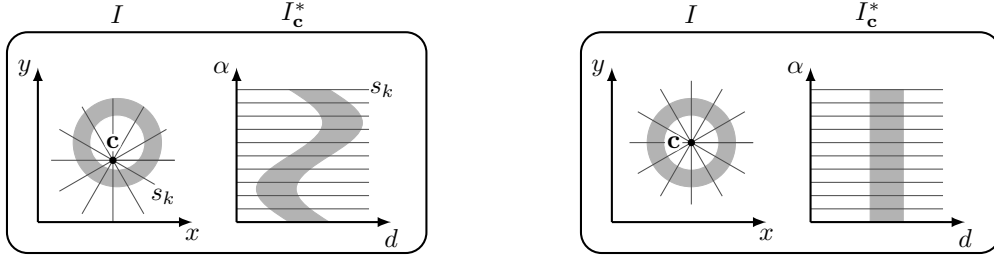
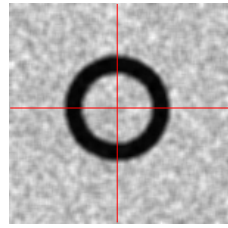
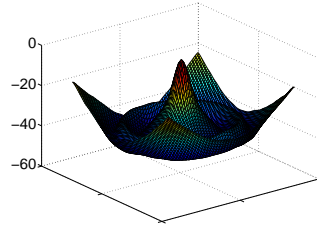


Figure 6. Transformation in (5) applied to an example image I . The intensities on the slices s_k are computed by bilinear interpolation. The accuracy of the transformation is determined by the number of equally spaced samples (with a distance d from the current centre) on each slice and the number of slices/angles α . For the centre on the left, $R(\mathbf{c})$ is large due to high variations of the intensities in direction α for given d , whereas the centre on the right is located correctly and $R(\mathbf{c})$ is almost 0 since there are no deviations vertically.



(a) low-pass filtered input image



(b) objective function $R(\mathbf{c})$

Figure 7. Centre localisation by radial symmetry for a exemplary image (left). The detected centre (left) corresponds to the position with the maximum value of the inverted objective function $R(\mathbf{c})$ (right).

reaches its minimum for the correct centre. Based on this observation, we define the notion of radial symmetry R for a particular centre \mathbf{c} in the image I by

$$R(\mathbf{c}) = \frac{1}{M} \sum_{i=1}^M \sqrt{\frac{1}{L} \sum_{j=1}^L (I_{\mathbf{c}}^*(i, j) - \mu_j)^2}, \quad (5)$$

with

$$I_{\mathbf{c}}^*(x, y) = I \left(\text{atan} \left(\frac{y - c_y}{x - c_x} \right), \|\mathbf{x} - \mathbf{c}\|_2 \right), \quad \text{and} \quad (6)$$

$$\mu_j = \frac{1}{M} \sum_{i=1}^M I^*(i, j), \quad (7)$$

where I^* is the polar transform of the image I with the origin located at \mathbf{c} , M is the number of slices, L is the number of samples on each slice and μ_j is the mean value of the j -th sample over all slices. A slice s is defined as the (grey level/colour) intensities along a particular orientation with a particular reference \mathbf{c} (see Fig. 6). The optimal centre \mathbf{c}^* is then obtained by

$$\mathbf{c}^* = \arg \min_{\mathbf{c}} R(\mathbf{c}). \quad (8)$$

Since an iterative scheme for solving the optimisation problem 8 cannot be derived in closed-form, we evaluate R on a predefined grid. Then, the grid position with the minimum R yields the optimal centre. An example of the objective function and the estimated centre is shown in Fig. 7.

3. RESULTS WITH SYNTHETIC IMAGES

For performance evaluation of the three approaches, we created an synthetic dataset with images of 150×150 pixels containing a randomly centred annulus or circle of fixed size. The grey values of the annulus/circle were uniformly distributed within the interval $[40, 70]$ and the grey values of the background within $[50, 80]$. Thus, the images contain white noise and the contrast is very low (see Fig. 8). We further added multiplicative noise (speckle) and motion blur. For each object and each type of noise we created 100 images, which gives in total a dataset of 600 images. We compared the performance of the different approaches by computing the mean Euclidean distance between the correct centre and the estimated centre as well as the standard deviation.

For the radial symmetry approach (Sec. 2.2) we set the number of iterations $t_{\max} = 100$ and the number of trials $m = 50$. For the variance-based approach (Sec. 2.3) we evaluated the corresponding objective function $R(\mathbf{c})$ for several centre candidates, *i.e.* positions with a maximum distance of 50 pixel to the image centre, and identified the centre with the minimum value of the objective function. Furthermore, we created 100 slices s_i with a length of 50 pixel, each containing 100 equally spaced positions.

The results for the 600 synthetic images are shown in Tab. 1. Obviously, for all approaches the performance for images containing an annulus is superior to images containing a circle. This holds for all types of noise and is due to the additional information of the inner border of the annulus.

For images containing white noise the Hough transform and the gradient-based approach yield almost the same performance with a mean error rate of approximately 1 pixel for images containing a circle and a mean error rate of 0.79 pixel for images containing an annulus. The approach based on radial symmetry significantly outperforms the other approaches with an mean error rate of 0.71 pixel (circle) and 0.07 pixel (annulus).

For images containing speckle noise the performance of all approaches decreases, but the symmetry-based approach yields significantly better results with a mean error of less than 1 pixel. The Hough transform and the gradient approach perform almost equal with an error of approximately 9.5 pixel. For annulus images, the gradient approach clearly outperforms the Hough transform, since the number of large image gradients is almost

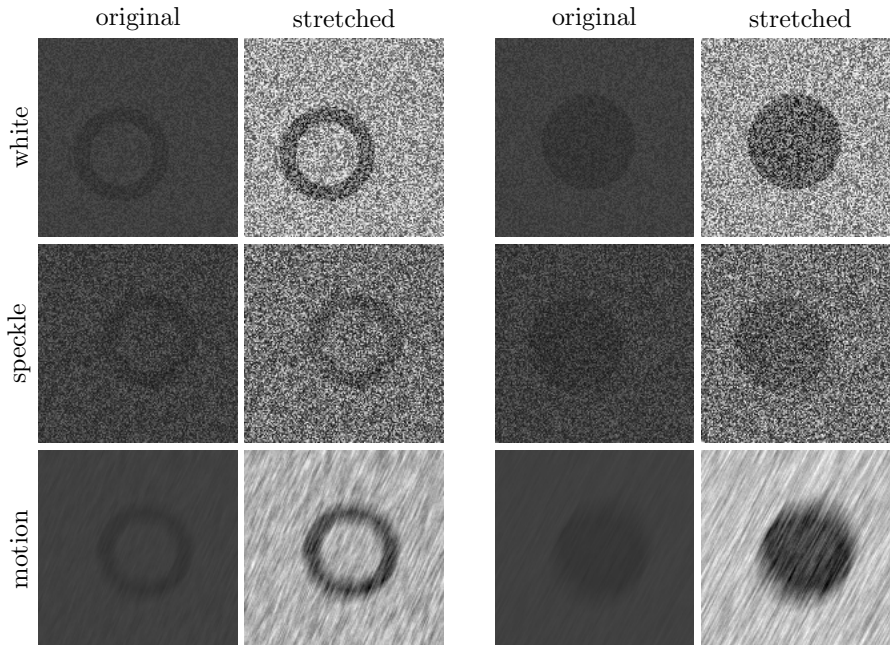


Figure 8. Example synthetic images containing an annulus or a circle with different types of noise: white noise, speckle noise, and motion blur. For comparison, the images are stretched to full range.

(a) white noise			(b) speckle noise	
method	circle	annulus	circle	annulus
Hough transform	0.91 (0.55)	0.79 (0.62)	9.89 (13.74)	9.39 (13.38)
gradient-based	1.01 (0.63)	0.78 (0.49)	8.70 (10.21)	4.64 (2.65)
radial symmetry	0.71 (0.11)	0.07 (0.16)	0.89 (0.71)	0.59 (0.55)

(c) motion blur		
method	circle	annulus
Hough transform	17.59 (16.44)	14.90 (14.54)
gradient	2.55 (1.66)	1.64 (1.35)
radial symmetry	0.52 (0.59)	0.21 (0.42)

Table 1. Mean error in pixel for centre localisation applied to synthetic images with low contrast and different kind of noise. The standard deviation is shown in brackets.

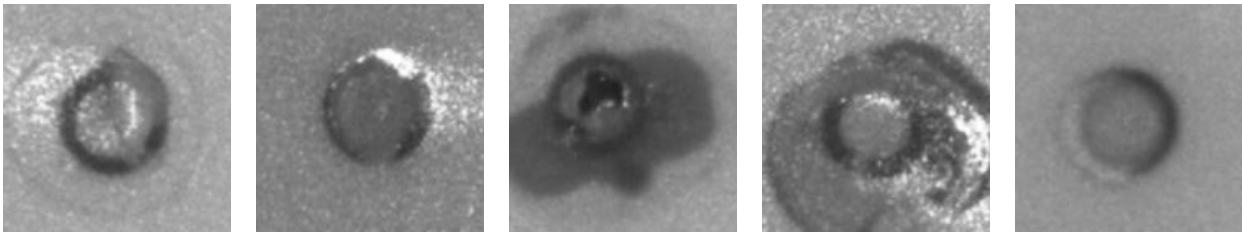


Figure 9. Example images of semi-conductor components for which the centre of the annulus has to be detected accurately for calibration purposes. The images contain different kinds of noise and the annulus can be partially occluded.

twice compared to images containing a circle. Thus, the gradient approach becomes more robust to speckle noise by this additional information.

For images with motion blur the object shape and the object contour partially changed such that the Hough transform cannot detect the correct centre (mean error 17.59 pixel for circles and 14.90 pixel for annuli). However, the gradient and the symmetry approaches yield accurate results. Since partial variations of the object shape and object contour can be compensated by the radial symmetry method, it outperforms significantly the other two methods with an error of 0.52 pixel for circles and 0.21 pixel for annuli.

In total, the radial symmetry approach achieves the best overall performance for noisy and low contrast images with an error of less than 1 pixel, and the gradient-based approach outperforms the Hough transform in all cases of higher image degradations.

4. RESULTS WITH REAL WORLD IMAGES

We further applied the proposed approaches to real world images, *e.g.* images of semi-conductor components with occlusions and strong noise (see Fig. 9). In total, this dataset consists of 82 images of size 120×120 pixel for which the centre of the annulus was labelled by experts. We applied the proposed approaches with the same parameter settings mentioned in the previous section and evaluated the Euclidean distance between the correct centre and the estimated centre.

Similar to the results for synthetic images, the radial symmetry approach significantly outperforms the other approaches with a mean error of 0.98 pixel, whereas the gradient approach yields an error of 2.16 pixel (see Tab. 2(a)). Since some of the annuli are partially occluded and affected by strong noise, the contour delivered by an edge detector doesn't really correspond to the contour of the annulus. Thus, the centre estimated by the Hough transform is incorrect.

The symmetry-based and the gradient-based approaches are robust to occlusion and strong noise for images of semi-conductor components, while preserving simplicity and efficiency. Both approaches yield superior performance concerning computation time compared to the Hough transform (see Tab. 2(b)). Moreover, using the

(a) error		(b) computation time (normalised)	
method	mean error (std.)	method	time (relative)
Hough transform	3.97 (5.65)	Hough transform	100 %
gradient	2.16 (2.52)	gradient	21 %
radial symmetry	0.98 (1.16)	radial symmetry	88 %

Table 2. Results for the three approaches for centre localisation applied to images of semi-conductor components. In (a), the accuracy is evaluated by the Euclidean distance between the estimated and the correct centre over 82 images. The computation time in (b) is normalised to the time the Hough transform requires.

gradient-based approach the computation time is significantly reduced by 79%, which holds also for the synthetic images of the previous section.

5. CONCLUSION

We have proposed two novel approaches for the precise centre localisation of LEDs. The first approach is based on the orientation of image gradients with a novel objective function, which is maximised by a simple and fast gradient ascend technique. Compared to existing approaches, we directly incorporate the potential centre into the objective function and obtain a very simple cost-function, which is based on dot products only. Hence, we avoid the exhaustive search and we can therefore compute the centre efficiently. The second approach is based on the definition of radial symmetry, for which we derive an objective function. Geometrically, given the optimal centre, the intensities along a circle with a certain radius vary only slightly. Therefore, the centre corresponds to the location where the mean variation of intensities over several radii reaches its minimum. We evaluate the accuracy and the runtime compared to an approach based on the Hough transform for different image datasets.

We created synthetic, low contrast images with a randomly centred annulus or circle of fixed size. Furthermore, we added three different kinds of noise: white noise, speckle noise, and motion blur. The radial symmetry approach achieves the best overall performance with a mean error of 0.76 pixel and the gradient-based approach outperforms the Hough transform in all cases of higher image degradations. We further applied the proposed approaches to detect the centre of p-electrodes of light emitting diodes with occlusions and strong noise. Again, the radial symmetry approach significantly outperforms the other approaches with a mean error of 0.98 pixel, whereas the gradient approach yields a significant improvement (2.16 pixel) compared to the Hough transform (3.97 pixel).

Concerning the computation time, the two novel approaches yield superior performance compared to the Hough transform as they reduce the computation time by 79% (gradient-based approach) and 12% (symmetry-based approach), respectively. Since the computation time of our approaches can easily be controlled by their parameters, *e.g.* the accuracy of the slices or the number of iterations, they can be applied to a wide range of applications such as eye tracking or object tracking in real-time. In industrial applications where the centre has to be estimated precisely, *e.g.* for precise calibration or inspection, the variance approach can provide the most accurate centre estimations.

REFERENCES

- [1] Hough, P. V. C., “Methods and means to recognize complex patterns,” U.S. Patent 3,069,654 (1962).
- [2] Duda, R. O. and Hart, P. E., “Use of the Hough transform to detect lines and curves in pictures,” *Communications of the ACM* **15**(1), 11–15 (1972).
- [3] Kimme, C., Ballard, D. H., and Sklansky, J., “Finding circles by an array of accumulators,” *Communications of the ACM* **18**(2), 120–122 (1975).
- [4] Minor, L. G. and Sklansky, J., “The detection and segmentation of blobs in infrared images,” *IEEE Trans. Systems, Man and Cybernetics* **11**, 194–201 (1981).
- [5] Ioannou, D., Huda, W., and Laine, A. F., “Circle recognition through a 2D Hough transform and radius histogramming,” *Image and Vision Computing* **17**(1), 15–26 (1999).

- [6] Kierkegaard, P., “A method for detection of circular arcs based on the Hough transform,” *Machine Vision and Applications* **5**, 249–263 (1992).
- [7] Illingworth, J. and Kittler, J., “A survey of the Hough transform,” *Computer Vision, Graphics, and Image Processing* **44**(1), 87–116 (1988).
- [8] Atherton, T. J. and Kerbyson, D. J., “Size invariant circle detection,” *Image Vision Comp.* **17**(11), 795–803 (1999).
- [9] Yuen, H. K., Princen, J. P., Illingworth, J., and Kittler, J. V., “Comparative study of Hough transform methods for circle finding,” *Image and Vision Comp.* **8**(1), 71–77 (1990).
- [10] Ceccarelli, M., Petrosino, A., and Laccetti, G., “Circle detection based on orientation matching,” in [*ICIAP*], 119–124, IEEE Computer Society (2001).
- [11] Lichtenauer, J., Hendriks, E. A., and Reinders, M. J. T., “Isophote properties as features for object detection,” in [*CVPR*], 649–654, IEEE Computer Society (2005).
- [12] Valenti, R. and Gevers, T., “Accurate eye center location and tracking using isophote curvature,” in [*CVPR*], IEEE Computer Society (2008).
- [13] Nocedal, J. and Wright, S. J., [*Numerical Optimization*], Springer-Verlag, New York (1999).